Copper(II) and manganese(II) complexes based on a new *N,O*-chelating ligand bearing the 1,3,5-diazaphosphorinane moiety*

K. R. Trigulova, A. V. Shamsieva, A. I. Kasimov, I. A. Litvinov, S. K. Amerhanova, A. D. Voloshina, E. I. Musina, and A. A. Karasik*

Arbuzov Institute of Organic and Physical Chemistry, FRC Kazan Scientific Center, Russian Academy of Sciences, 8 ul. Akad. Arbuzova, 420088 Kazan, Russian Federation.
Fax: +7 (843) 273 2253. E-mail: kamtri95@mail.ru

Copper(II) and manganese(II) chelate complexes were synthesized using the new *N,O*-hybrid ligand 1,3-dibenzhydryl-5-(pyridin-2-yl)-1,3,5-diazaphosphinane 5-oxide. The synthesized complexes were characterized by physicochemical methods. The molecular and crystal structures of the complexes were established by X-ray diffraction. All new compounds were evaluated for cytotoxicity against the cancer cell lines M—HeLa and HuTu80 and the normal cell line Chang liver.

Key words: diazaphosphorinane, pyridyl-containing phosphine oxides, *N,O*-chelating ligands, Cu^{II} complexes, Mn^{II} complexes, cytotoxicity, molecular structure, X-ray diffraction analysis.

In the past decades, transition metal complexes have attracted great attention as potential antitumor agents.[1,2] Despite tremendous success of agents based on platinum complexes in the treatment of different cancer tumors,[3—5] serious adverse effects restrict the use of these compounds.[3,6,7] Therefore, in the cancer therapy there is a continuous urgent need for the development of alternative chemotherapeutic agents based on metals other than platinum, which would exhibit improved pharmacological properties and high selectivity of cytotoxic action.

Compared to platinum complexes, complexes of the metals that are present in the human body, such as copper, cobalt, manganese, nickel, and zinc, can have higher biocompatibility and lower toxicity, due to which they can be considered as promising components of antitumor agents.[8—12] The Mn^{II} and Cu^{II} ions play a key role in the oxygen metabolism in many biological systems,[13,14] and their complexes can influence the translation and transcription of double-stranded DNA. The Mn^{II} complexes exhibit anticancer/antiproliferative activity. Copper complexes play an important role in the endogenous oxidative DNA damage accompanying aging,[15,16] and these complexes are potential anticancer agents as efficient as platinum complexes but less toxic.[17,18] Therefore, we chose transition metal ions (Mn^{II} and Cu^{II}) for the synthesis of new complexes.

The nature of ligands is also closely related to the biological activity of metal complexes.[19] Recently, we have demonstrated that copper complexes based on *N,O*-hybrid ligands, pyridyl-containing phospholane oxides, exhibit cytotoxic activity comparable with that of the standard anticancer drug tamoxifen.[20] The variation of the substituent at the phosphorus atom, the ring size, and the conformational rigidity of the structure can affect the cytotoxic properties of the ligand and transition metal complexes with this ligand. In this work, we chose the *N,O*-hybrid ligand containing the six-membered 1,3,5-diazaphosphorinane heterocycle, used it to construct copper(II) and manganese(II) complexes, determined their structures, and studied their physicochemical properties. All new compounds were evaluated for cytotoxicity against the cancer cell lines M—HeLa and HuTu80 and the normal cell line Chang liver.

Results and Discussion

Synthesis of ligand L. The starting cyclic 1,3-dibenzhydryl-5-(pyridin-2-yl)-1,3,5-diazaphosphorinane was synthesized by the known procedure based on the condensation of (2-pyridyl)phosphine, paraformaldehyde, and diphenylmethylamine.[21] The subsequent oxidation

* Dedicated to Academician of the Russian Academy of Sciences V. I. Ovcharenko on the occasion of his 70th birthday.

Published in Russian in *Izvestiya Akademii Nauk. Seriya Khimicheskaya,* No. 7, pp. 1410—1421, July, 2022.

of the resulting tertiary phosphine with a 30% aqueous hydrogen peroxide solution in acetone afforded target phosphine oxide **L** (Scheme 1).

Scheme 1

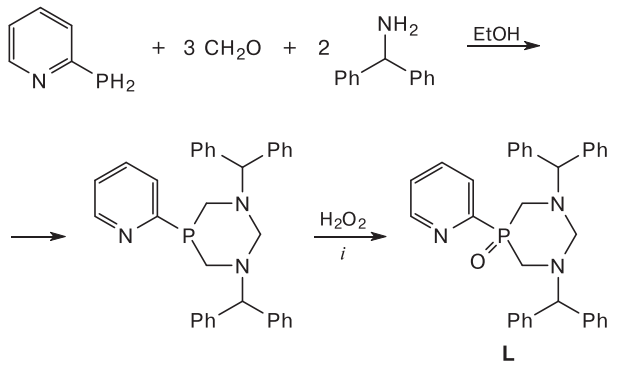

i. Acetone.

Phosphine oxide **L** is a white powder readily soluble in most organic solvents. The composition of this compound was determined by mass spectrometry and elemental analysis. The ESI mass spectrum of compound **L** shows the presence of ions at m/z 530 and 552 corresponding to $[M + H]^+$ and $[M + Na]^+$, respectively. The structure of phosphine oxide **L** was confirmed by NMR and IR spectroscopy. The characteristic vibrations of the phosphoryl group in the IR spectrum at 1174 cm^{-1} are indicative of the formation of phosphine oxide. The ^{31}P NMR spectrum shows one signal at δ_P 18.5 characteristic of cyclic tertiary phosphine oxides. In the ^1H NMR spectrum, the protons of the pyridyl moiety appear as four groups of signals at δ_H 7.34, 7.77, 8.05, and 8.68. The signals of phenyl groups are observed at δ_H 7.08—7.42. The methylene protons of the heterocycle resonate as four multiplets at δ_H 3.21—3.86. The methine protons of the benzhydryl substituents appear as a singlet at δ_H 5.08.

The structure of compound **L** was confirmed by single-crystal X-ray diffraction. The single crystals of compound **L** suitable for X-ray diffraction were obtained by slow concentration of a saturated solution of compound **L** in ethanol at room temperature. We obtained two types of crystals, which differ in the shape and size (**L1** and **L2**). According to the X-ray diffraction analysis, these crystals are isostructural crystal solvates of compound **L** with water (**L1**) and simultaneously with water and ethanol (double solvate **L2**). Since the crystals of **L1** and **L2** are isostructural, the crystal structure of **L2** was established at low temperature, and the geometric parameters of the molecule were determined with a lower error, the conformation and other geometric parameters of molecule **L** are discussed in relation to the molecule in the crystal of **L2** (Fig. 1).

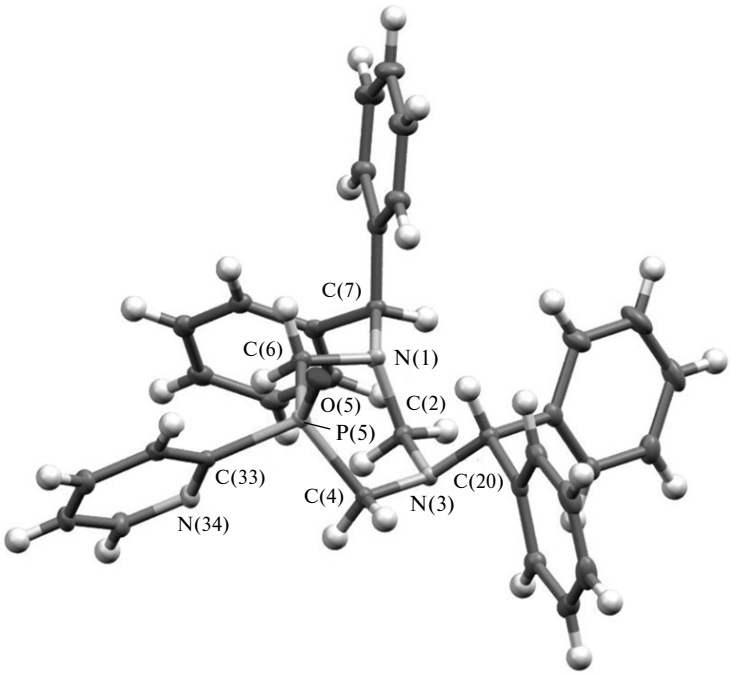

Fig. 1. Molecular structure of compound **L** in crystal **L2** with displacement ellipsoids drawn at the 50% probability level. Water and ethanol solvent molecules are omitted for clarity.

The six-membered heterocycle of molecule **L** adopts a chair conformation, like the previously studied related 1,3-dibenzyl-5-phenyl-1,3,5-diazaphosphorinane containing the unoxidized phosphorus atom.[22] The phosphorus atom has a tetrahedral coordination environment, with the pyridine substituent at this atom being in the equatorial position (like the phenyl substituent in the 1,3-dibenzyl-5-phenyl-1,3,5-diazaphosphorinane molecule) and the phosphoryl group being in the axial position. The nitrogen atoms bonded to the sp^3-hybridized carbon atoms have a trigonal-pyramidal geometry (the sums of the bond angles are 335.8(1) and 336.7(1)°). The benzhydryl substituents at the N(1) and N(3) atoms are in the equatorial and axial positions, respectively. The N—C bond lengths in these molecules are equal within experimental error. The main geometric parameters (bond lengths and bond angles) of molecules **L** in the crystals (**L1** and **L2**) have values typical of the corresponding moieties (phosphine oxides and aromatic substituents). The packing of the isostructural crystals (**L1** and **L2**) is stabilized by hydrogen bonds and van der Waals interactions. In the crystals, molecules **L** and the solvent molecules are connected *via* van der Waals interactions to form dimers (Fig. 2).

In the crystal of **L1**, there is also a similar dimer formed through bridging water molecules, but ethanol molecules are absent.

Synthesis of copper(II) and manganese(II) complexes. Complexes **1—3** were synthesized in good yields by the reaction of ligand **L** with $CuCl_2 \cdot 2H_2O$, $Cu(BF_4)_2 \cdot H_2O$, or $MnCl_2$, respectively, in ethanol in stoichiometric ratios given in Scheme 2.

Complexes **1—3** are readily soluble in most organic solvents; compounds **1** and **2** are also soluble in water. The compositions of the complexes were confirmed by mass spectrometry and elemental analysis. The mass spectrum of complex **1** shows a fragment ion peak at m/z 631 corresponding to the composition $[CuLCl]^+$. Complex **2** gives fragment ion peaks at m/z 592 and 1121 corresponding to the compositions [CuL] and $[CuL_2]$, respectively. The MALDI mass spectrum of complex **3** shows a single fragment ion at m/z 1149 corresponding to the composition $[MnL_2Cl]^+$.

The IR spectra of complexes **1—3** were compared with the spectra of free ligand **L** in order to determine the involvement of potential donor sites in the coordination. The coordination of the phosphoryl group is confirmed by the lower frequencies of the absorption bands corresponding to P=O stretching vibrations in the IR spectra of complexes **1—3** (1168, 1152, and 1153 cm^{-1}, respectively) compared to the free ligand (1174 cm^{-1}).[23,24] The absence of $\nu(H_2O)$ and the bands of ethanol in the spectra of complexes **1—3** is indicative of the replacement of coordinated water molecules in the starting compounds $CuCl_2 \cdot 2H_2O$ and $Cu(BF_4)_2 \cdot H_2O$ by the phosphine oxide ligand. The intense bands at 1075 cm^{-1} in the spectrum of complex **2** are assigned to vibrations of the tetrafluoroborate anion. According to the mass spectrometry results, elemental analysis data, and the IR spectrum, complex

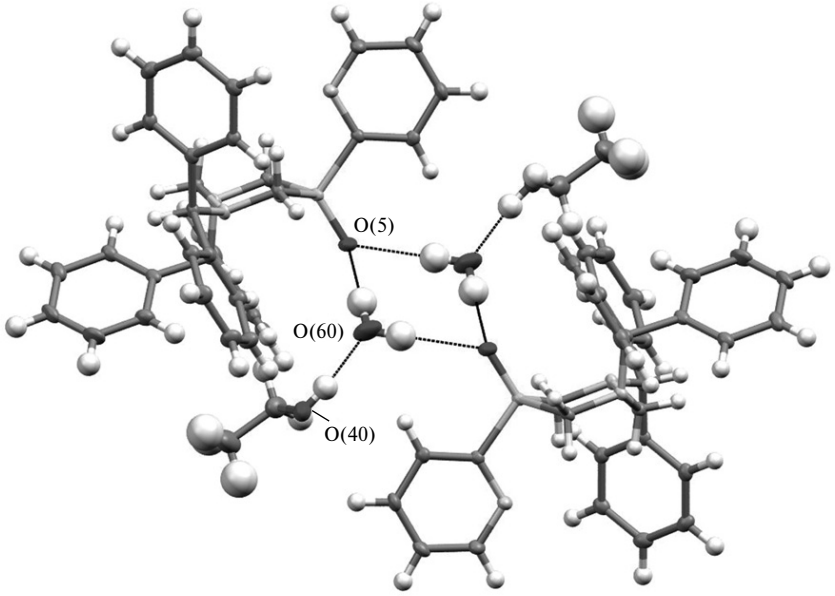

Fig. 2. Hydrogen bond system in crystal **L2**.

Scheme 2

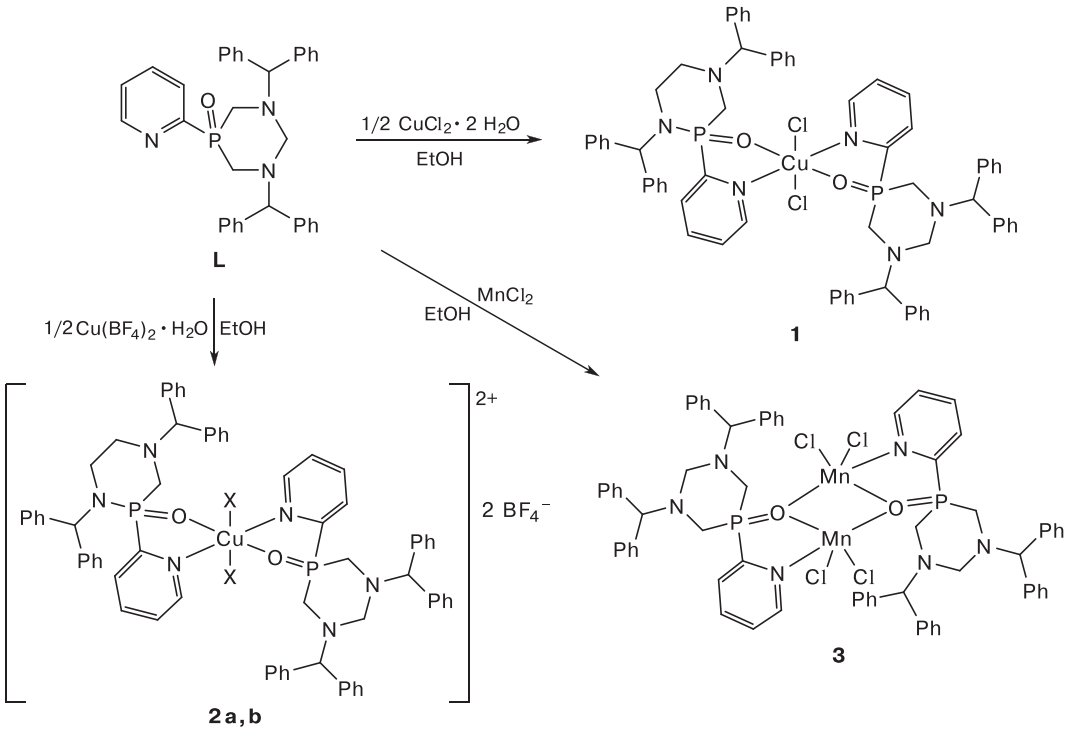

X = EtOH (**2a**), MeCN (**2b**)

2 initially had the composition $[CuL_2](BF_4)_2$, but its recrystallization from ethanol or acetonitrile resulted in the formation of single crystals of complexes **2a** and **2b**, in which two solvent molecules act as co-ligands, as was determined by X-ray diffraction analysis. The structures of complexes **1** and **3** were also established by single-crystal X-ray diffraction.

Single crystals of compound **1** were obtained by slow concentration of its saturated solution in acetonitrile at room temperature. Single crystals of complex **3** suitable for X-ray diffraction were obtained by slow concentration of a saturated solution of the complex in the chloroform—hexane system.

Copper complexes **1**, **2a**, and **2b** are similar. Complexes **2a** and **2b** form isostructural crystals. Complex **1** crystallizes as a solvate with ethanol and water. In the crystals, the molecules of complexes **1**, **2a**, and **2b** are in special positions. The copper atoms lie on inversion centers, and the ligands and co-ligands are coordinated to the Cu atoms in a symmetric mode to form an octahedral environment. The molecular structure of complex **1** is shown in Fig. 3; that of complex **2b**, in Fig. 4. The crystal structure of manganese complex **3** contains two independent molecules, each being in a special position on an inversion center. Since the crystallographically independent molecules are structurally identical, Figure 5 shows the molecular structure of one molecule.

In complexes **1—3**, the pyridylphosphine oxide ligand is coordinated to the metal ions through the pyridyl nitrogen atom and the phosphoryl oxygen atom in a chelating mode. The N—M—O chelate angle in the copper complexes varies in the range of 83.12(5)—87.24(7)°; in the manganese complex, in the range of 76.3(2)—76.9(2)°. Selected bond lengths and bond angles in complexes **1—3** are given in Table 1.

Due to the centrosymmetric structures of complexes **1**, **2a**, and **2b**, the coordinating heteroatoms of two ligands of the same nature are in *trans* positions with respect to the metal ion. All atoms of the five-membered *N,O*-chelate metallocycles formed through coordination, except for the oxygen atoms, are nearly in one plane. The deviation of the oxygen atoms in different directions from the NCPCuNCP plane is 0.520, 0.303, and 0.184 Å in compounds **1**, **2a**, and **2b**, respectively, and it correlates with the size of the heteroatom in the coordinating co-ligand. The octahedral coordination environment of the copper atoms is completed by either

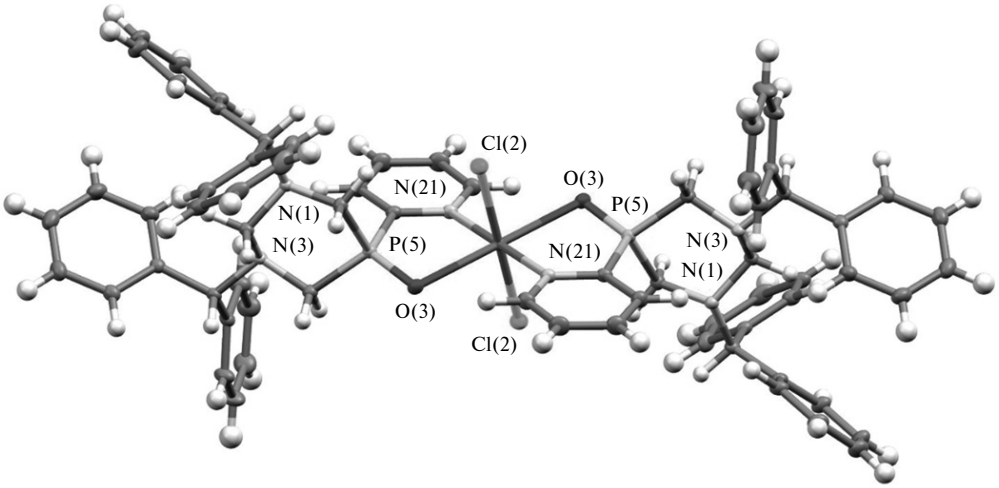

Fig. 3. Molecular structure of complex **1** in the crystal with displacement ellipsoids drawn at the 50% probability level. Water and ethanol solvent molecules are omitted for clarity.

chlorine atoms (complex **1**) or the solvent molecules EtOH (**2a**) or MeCN (**2b**) in the apical position. The Cu—Cl, Cu—O, and C—N bond lengths are 2.3369(4), 2.423(2), and 2.520(2) Å for complexes **1**, **2a**, and **2b**, respectively, and they also correlate with the size of the coordinating donor atom. The P=O bond length in the complexes is larger compared to that in the free ligand and varies from 1.495(1) to 1.505(2) Å (1.488(2) Å in the free ligand). It should be noted that the P=O bond length correlates well with the shift of the characteristic P=O stretching band in the IR spectra. Thus, this band is bathochromically shifted by 6—21 cm^{-1} with increasing bond length.

As opposed to copper complexes **1**, **2a**, and **2b**, manganese complex **3** is binuclear and has a dimeric centrosymmetric structure. In the crystal of complex **3**, the manganese atoms do not lie on symmetry elements. In this complex, ligands **L** are bridging, the oxygen atom of the phosphoryl group being coordinated to two manganese atoms. The manganese(II) ion has a

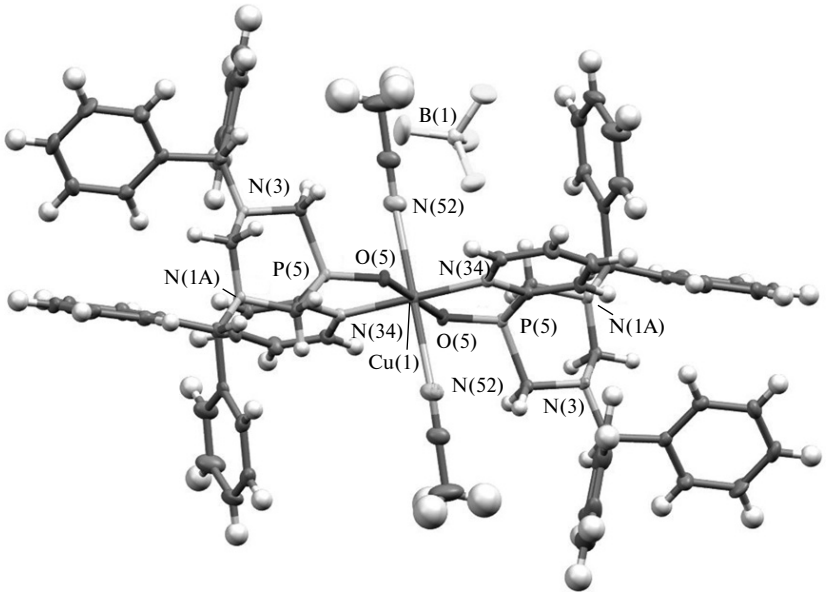

Fig. 4. Molecular structure of complex **2b** in the crystal with displacement ellipsoids drawn at the 50% probability level. Acetonitrile solvent molecules and the second BF_4 anion are omitted for clarity.

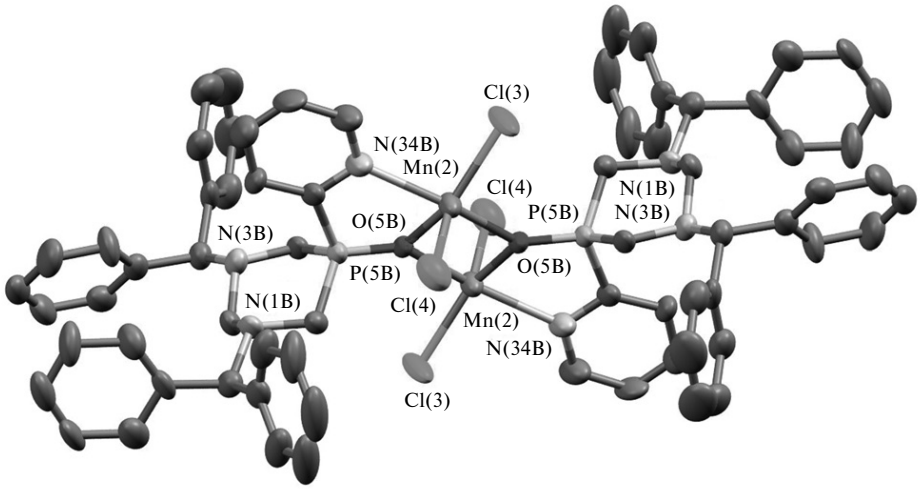

Fig. 5. Molecular structure of complex **3** (independent molecule **B**) in the crystal with displacement ellipsoids drawn at the 50% probability level. Chloroform solvent molecules and H atoms are omitted for clarity.

Table 1. Selected bond lengths (*d*) and bond angles (ω) in complexes **1**—**3**

Parameter	**1**	**2a**	**2b**	**3**[a]
Bond		*d*/Å		
Cu—E[b]	2.3369(4)	2.4232(19)	2.520(2)	—
P=O[c]	1.4951(12)	1.5127(16)	1.5050(15)	1.507(5) 1.506(5)
$M—N_{Py}$[d]	2.0034(13)	2.0033(19)	1.9968(18)	2.251(7) 2.262(7)
$M—O_{P=O}$[d]	2.3584(11)	1.9685(16)	1.9691(13)	2.201(5) 2.215(6)
Angle		ω/deg		
$O_{p=o}—M—N_{Py}$[d]	83.12(5)	87.24(7)	86.98(6)	76.9(2) 76.3(2)
$O_{p=o}—Mn—O_{p=o}$	—	—	—	74.4(2) 74.8(2)

[a] The values are given for two independent molecules.
[b] E = Cl (**1**), O_{EtOH} (**2a**), N_{MeCN} (**2b**).
[c] The P=O bond length in free ligand **L** is 1.488(2) Å.
[d] M = Cu (**1**, **2a**, **2b**), Mn (**3**).

trigonal-bipyramidal coordination. The chlorine atoms and the phosphoryl oxygen atom occupy equatorial positions; the oxygen atom of the symmetry-related ligand and the pyridyl nitrogen atom are in apical positions. In complex **3**, due to the bridging coordination of the chelating ligands, the $Mn—O_{P=O}$ bond length is larger (2.201(5) and 2.215(6) Å in two independent molecules) compared to those typical of manganese(II) chelate complexes.[25,26]

Of particular note are the conformational changes of the ligand in complexes **1**—**3** compared to free ligand **L**. In ligand **L**, the pyridyl substituent at the phosphorus atom is in the equatorial position, the benzhydryl substituent at one nitrogen atom is also in the equatorial position, and the benzhydryl substituent at another nitrogen atom is in the axial position. In all complexes, the heterocycle retains the chair conformation, but the pyridyl substituents at the phosphorus atoms are in axial positions, whereas both benzhydryl substituents are in equatorial orientations.

Compound **3** crystallizes as a solvate with a large number of chloroform molecules, some of which are disordered by symmetry elements and were not experimentally located. In the crystal, there are large

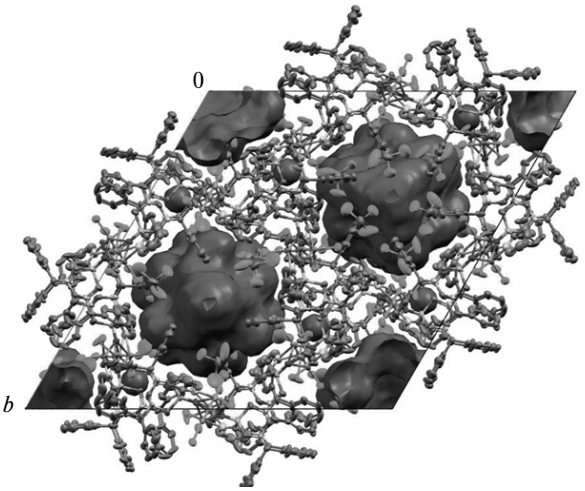

Fig. 6. Unit cell of the crystal of complex **3** projected along the *c* axis. The void space in the crystal accessible for small molecules is highlighted in dark gray.

voids, which can be occupied by these molecules (Fig. 6).

The unit cell volume of **3** is 39033(9) Å^3, the void space being 6529 Å^3 (17%). The calculation of the disordered solvent contribution by the PLATON SQUEEZE tool demonstrated that these voids can contain molecules with 2370 electrons. In the unit cell of the crystal of **3**, there are 18 molecules of complex **3** and 54 located and refined chloroform molecules (three solvent molecules per complex); also the unit cell can contain up to 46 chloroform molecules that were not located.

Due to these crystal structure features, compound **3** can be used to construct porous materials with high adsorption capacity.

Cytotoxic activity. Uncontrolled side effects due to the absence of selectivity of most of the present-day chemotherapeutic drugs for cancer therapy are a constant challenge. Many popular chemotherapeutic drugs have good cytotoxicity but low selectivity.[27] The selectivity of compounds against cancer cells is an important parameter for the evaluation of cytotoxic activity characterized by the selectivity index (SI).

Compounds **L** and **1—3** were evaluated for cytotoxicity against the human normal (Chang liver) and cancer (M—HeLa and HuTu80) cell lines. The results are summarized in Table 2.

The IC_{50} value of **L** against the cancer cell lines M—HeLa and HuTu80 is much lower compared to those of tamoxifen and 5-fluorouracil used as standard cancer drugs. The IC_{50} value of **L** against the normal Chang Liver cells is similar to that of tamoxifen, but ligand **L** is more cytotoxic compared to 5-fluorouracil.

According to the IC_{50} values, the chelation to the metal ion selectively enhances the cytotoxicity of ligand **L** against the cancer cells M—HeLa but also increases the cytotoxicity against the normal Chang liver cells. Complexes **1** and **3** are lead compounds against the cell line M—HeLa, with the IC_{50} values of 14.4 and 13.8 μmol L^{-1}, respectively. All complexes **1—3** exhibit lower cytotoxicity against the HuTu80 cells compared to ligand **L**. Complexes **2** and **3** with IC_{50} of 18.6 and 21.0 μmol L^{-1}, respectively, are lead compounds against the cell line HuTu80 compared to 5-fluorouracil.

Compounds with SI $\geqslant$ 3 are assumed to be highly selective.[28] Therefore, compound **L** is highly selective against the cell line HuTu 80 (SI = 5.0). Complex **2** has a lower selectivity (SI = 2.3) compared to free ligand **L**, but its selectivity index is higher than that of 5-fluorouracil (SI = 1.3).

Therefore, we used the new ligand 1,3-dibenzhydryl-5-(pyridin-2-yl)-1,3,5-diazaphosphinane 5-oxide to synthesize neutral and cationic mononuclear Cu^{II} complexes and the binuclear Mn^{II} complex with the ligand coordinated in the *N,O*-chelating mode. These

Table 2. Cytotoxic properties (μmol L^{-1}) and the selectivity indices (SI) of phosphine oxide **L** and its complexes **1—3**

Compounds	Cancer cell lines				Normal cell line Chang liver
	M—HeLa		HuTu80		
	IC_{50}	SI	IC_{50}	SI	IC_{50}
L	24.5±1.9	1.9	9.4±0.7	5.0	46.3±3.7
$[CuL_2Cl_2]$ (**1**)	14.4±1.3	1.3	63.3±5.2	0.3	19.0±1.6
$[CuL_2](BF_4)_2$ (**2**)	42.8±3.4	1.0	18.6±1.5	2.3	43.5±3.5
$[Mn_2L_2Cl_4]$ (**3**)	13.8 ±1.2	1.3	21.0±1.7	0.8	17.4±1.4
Tamoxifen	28.0±2.5	1.7	—	—	46.2±3.5
5-Fluorouracil	62.0±4.7	1.4	65.2±5.4	1.3	86.3±6.5

Note. The experiments were performed in triplicate. The results are given as the mean value ± standard deviation (SD).

complexes are paramagnetic with an octahedral or trigonal-bipyramidal coordination environment of the metal center. The crystal structure of the Mn^{II} complex was found to have a large void space (17%), due to which it can be used to construct porous materials with high adsorption capacity.

The evaluation of the cytotoxic activity of phosphine oxide **L** and complexes **1—3** demonstrated that ligand **L** and copper complexes **1** and **2** exhibit higher cytotoxicity against the cell line M—HeLa compared to the reference compounds tamoxifen and 5-fluorouracil. Ligand **L** and complexes **2** and **3** proved to be efficient against the cell line HuTu80. Complexes **1** and **3** were found to be more cytotoxic against the normal Chang liver cells compared to tamoxifen and 5-fluorouracil, whereas the IC_{50} values of compounds **L** and **2** are nearly equal to that of tamoxifen.

The results of this study and the synthetic accessibility of 1,3,5-diazaphosphorinane P-oxides provide a route to the fine tuning of the properties of their copper and manganese complexes, including the modification of their adsorption capacity and cytotoxicity, by varying the substituents at the nitrogen atoms with the retention of the metal core.

Experimental

All starting metal derivatives were commercially available reagents. The solvents were purified and dried immediately before use. Starting 1,3-dibenzhydryl-5-(pyridin-2-yl)-1,3,5-diazaphosphorinane was synthesized by a procedure described previously.[21] Complex **3** was synthesized under an inert atmosphere using a vacuum argon line.

The NMR spectra were recorded on a Bruker Avance-400 spectrometer (^1H, 400 MHz; ^{31}P, 162 MHz). The ^1H NMR chemical shifts are given with respect to the residual signal of the solvent $CDCl_3$ (δ_H 7.27). The ^{31}P NMR chemical shifts are given with respect to the signals of H_3PO_4 (85%) as the external standard (δ_P 0.0).

The IR spectra were measured on a Bruker Tensor 27 spectrometer (Germany) in the wavelength range from 4000 to 400 cm^{-1} as Nujol mulls. The measurements were preformed and the spectra were processed and evaluated using the OPUS 7/2012 software.

Electrospray ionization-ion-trap mass spectra (ESI-MS) were obtained on an AmazonX mass spectrometer (Bruker Daltonik GmbH, Germany) in positive (and/or negative) ion mode at m/z in the range from 70 to 3000. The capillary voltage was −3500 V. Nitrogen was used as the drying gas with a temperature of 250 °C and a flow rate of 10 L min^{-1}. A methanol—water mixture (70 : 30, v/v) was used as the eluent, with a flow rate of 0.2 mL min^{-1} (Agilent 1260 chromatograph, USA). The analyte was dissolved in methanol at a concentration of 10^{-6} g L^{-1}. The sample was injected into the flow system through a Rheodyne 7725 injection valve (Rheodyne, USA). The sample injection volume was 20 μL. The mass spectrometric parameters were controlled and the data were acquired using the TrapControl 7.0 software (Bruker Daltonik GmbH, Germany). The data were processed with the DataAnalysis 4.0 SP4 software (Bruker Daltonik GmbH, Germany). The MALDI mass spectra were acquired in linear positive-ion mode on an Ultraflex III TOF/TOF mass spectrometer (Bruker Daltonik GmbH, Germany) equipped with a Nd:YAG laser (λ = 355 nm, the frequency was 100 Hz). The mass spectrum was obtained with an accelerating voltage of 25 kV and an extraction delay time of 30 ns. The resulting mass spectrum was formed by multiple laser irradiation of the crystal (50 laser pulses). A 1% solution of the matrix in acetonitrile (0.5 μL) and a 0.1% solution of the sample in methanol (0.5 μL) were sequentially deposited onto the metal target MTP AnchorChipTM and then evaporated. The data were obtained using the FlexControl software (Bruker Daltonik GmbH, Germany) and processed with the FlexAnalysis 3.0 software (Bruker Daltonik GmbH, Germany).

X-ray diffraction analysis. The X-ray diffraction data for the crystals of **L2**, **1**, and **2a** were collected on an automated Bruker D8 QUEST three-circle diffractometer equipped with a PHOTON III area detector and an IμS DIAMOND.0 microfocus X-ray tube (λ[Mo-$K\alpha$] = 0.71073 Å) at low temperatures given in Tables 3 and 4. The crystals of **L1** and **2b** were studied on a Bruker Kappa ApexII diffractometer (λ[Mo-$K\alpha$] = 0.71073 Å) at room temperature (293(2) K) and at a low temperature (100(2) K). The crystal of **3** was studied on the same diffractometer at room temperature (296(2) K). The X-ray diffraction data were collected and processed using the APEX3 software package. The structures were solved by direct methods using the SHELXT program[29] and refined by the full-matrix least-squares method based on F^2 using the SHELXL program.[30] Nonhydrogen atoms were refined with anisotropic displacement parameters. The hydrogen atoms at oxygen atoms were found in difference Fourier maps. The other hydrogen atoms were positioned geometrically and refined using a riding model. The crystals of **L1** and **L2** are isostructural. The former one is a crystal hydrate, and **L2** is a mixed solvate with water and ethanol. The ethanol molecule is disordered over two positions with site occupancies of 0.34 and 0.66. In the crystal of compound **1**, water and ethanol solvent molecules were also located. The ethanol molecule is disordered over two positions; one of these positions is located near a center of symmetry and is additionally disordered. The refinement of the site occupancies of the ethanol molecule gave the fractional value, *i.e.*, there are two water molecules and 1.423 ethanol molecule per molecule of the complex. In the crystal of **1**, the complex is in a special position on an inversion center. The crystals of **2a** and **2b** are also isostructural despite the fact that, as opposed to the crystal of **2a**, the crystal of **2b** contains acetonitrile solvent molecules. In the crystal structures, the cations of complexes **2a** and **2b** are in special positions on inversion centers. The stoichiometry of the crystal of **2b** is as follows: there are two BF_4^- anions, two water molecules, and 3.152 acetonitrile molecules per dication of the complex. The

crystal of compound **3** is trigonal centrosymmetric; the space group is *R*-3. Upon cooling on the diffractometer, the crystals underwent degradation and did not withstand low temperatures. Therefore, the X-ray diffraction data were collected at room temperature from a crystal, which was coated with fluoride varnish to prevent solvent loss. The asymmetric unit of the crystal contains two independent molecules of the complex, each molecule being in a special position on an inversion center. Formally, the asymmetric unit of the crystal contains one molecule of the complex and three chloroform solvent molecules. Difference electron density maps revealed intense peaks on a threefold inversion axis and nearby. Attempts to assign these peaks to chloroform molecules or other solvent molecules, that were used in the synthesis, failed. The atoms were arranged in random associates with unrealistic values of the anisotropic displacement parameters and interatomic distances. Therefore, we refined the structure using the SQUEEZE routine in the PLATON software package,[31] which takes into account an uncertain solvent during the structure refinement. The unit cell volume of the crystal of **3** is 39033(9) Å^3, with the void space being 6529 Å^3 (17%). According to the results of calculations, this void space can be filled by solvent molecules with 2370 electrons. The unit cell of the crystal of **3** contains 18 molecules of complex **3** and 54 located and refined chloroform molecules (3 solvent molecules per molecule of the complex); besides, the unit cell can contain up to 46 chloroform molecules that were not located. Due to high solvation, the crystals are air-unstable and undergo degradation on cooling. Therefore, the X-ray diffraction data were collected at room temperature from the crystal coated with fluoride varnish. This led to a low accurcacy of the determination of the main geometric parameters of the structure. The crystallographic data for these structures are given in Tables 3 and 4. The molecular and crystal structures were analyzed using the PLATON program.[32] The figures were produced using the MERCURY program.[33]

The crystallographic data for the structures were deposited with the Cambridge Crystallographic Data Centre. The CCDC refcodes and principal crystallographic data are given in Tables 3 and 4.

Table 3. Principal crystallographic data for **L1** and **L2**

Parameter	**L1**	**L2**
Molecular formula	$C_{34}H_{32}N_3OP$, H_2O	$C_{34}H_{32}N_3OP$, H_2O, C_2H_6O
Empirical formula	$C_{34}H_{34}N_3O_2P$	$C_{36}H_{40}N_3O_3P$
Molecular weight	547.61	593.68
Crystal system	Triclinic	Triclinic
Space group	$P\bar{1}$	$P\bar{1}$
T/K	293	100(2)
a/Å	9.7141(5)	9.5298(13)
b/Å	12.2290(6)	11.7665(15)
c/Å	13.2071(6)	14.383(2)
α/deg	108.062(2)	98.794(7)
β/deg	96.899(2)	102.600(7)
γ/deg	92.247(2)	96.792(7)
V/Å^3	1475.94(13)	1536.1(4)
Z/Z'	2/1	2/1
d_{calc}/g cm^{-3}	1.232	1.284
μ/mm^{-1}	0.128	0.131
F(000)	580	632
θ/deg	1.6—25.5	2.10—29.70
Number of reflections		
measured	66270	48500
unique	5386	8244
observed ($I > 2\sigma(I)$)	4137	5821
Goodness of fit	1.029	0.682
R ($I > 2\sigma(I)$)		
R_1	0.0417	0.0507
wR_2	0.0915	0.1372
R (based on all reflections)		
R_1	0.0615	0.0837
wR_2	0.1019	0.1729
Residual electron density (ρ_{max}/ρ_{min})/e Å^{-3}	0.26/−0.25	0.37/−0.35
CCDC	2161043	2161044

Note. **L1** is a crystal hydrate, **L2** is a crystal solvate with water and ethanol; the ethanol molecule is disordered.

Table 4. Principal crystallographic data for complexes **1—3**

Parameter	**1**	**2a**	**2b**	**3**
Molecular formula	$C_{68}H_{64}Cl_2CuN_6O_2P_2 \cdot 1.423C_2H_6O \cdot 2H_2O$	$C_{72}H_{76}CuN_6O_4P_2^+ \cdot 2BF_4^-$	$C_{72}H_{70}CuN_8O_2P_2^{2+} \cdot 2BF_4^- \cdot 3.152C_2H_3N$	$C_{68}H_{64}Cl_4Mn_2N_6O_2P_2 \cdot 3CHCl_3$
Molecular weight	316.41	1388.50	1507.79	1668.98
Crystal system	Triclinic	Monoclinic	Monoclinic	Trigonal
Space group	$P\bar{1}$	$P2_1/n$	$P2_1/n$	$R\bar{3}$
T/K	110(2)	104(2)	100	296(2)
a/Å	8.9553(4)	16.5275(6)	16.6775(12)	33.022(3)
b/Å	11.4900(5)	10.7416(3)	11.2020(8)	33.022(3)
c/Å	17.6639(8)	19.9724(6)	20.0970(14)	41.333(4)
α/deg	91.574(2)	—	—	90
β/deg	94.354(2)	95.568(1)	93.635(3)	90
γ/deg	111.086(2)	—	—	120
V/Å^3	1688.02(13)	3529.01(19)	3747.05(5)	39033(9)
Z/Z'	1/0.5	2/0.5	2/0.5	18
d_{calc}/g cm^{-3}	1.274	1.307	1.337	1.278
μ/mm^{-1}	0.504	0.428	0.409	0.771
F(000)	680	1446	1569	15336
θ/deg	1.90—30.00	2.20—28.00	3.0—28.8	1.5—28.4
Number of reflections				
measured	139114	149760	58072	216632
unique	9831	8492	7173	21743
observed ($I > 2\sigma(I)$)	8317	6731	5603	6924
Goodness of fR	1.05	1.07	1.025	1.102
R ($I > 2\sigma(I)$)				
R_1	0.0427	0.0544	0.0400	0.1236
wR_2	0.1153	0.1359	0.0873	0.2987
R (based on all reflections)				
R_1	0.0519	0.0708	0.0592	0.3025
wR_2	0.1207	0.1444	0.0953	0.4264
Residual electron density (ρ_{max}/ρ_{min})/e Å^{-3}	1.29/−1.08	1.57/−1.48	0.57/−0.41	2.77/−1.12
CCDC	2161045	2161046	2161047	2161050

Note. Complex **1** (empirical formula $C_{70.85}H_{76.54}Cl_2CuN_6O_{5.42}P_2$) is a crystal solvate with water and ethanol; the disordered ethanol molecule has a fractional occupancy; complex **2a** ($C_{72}H_{76}CuN_6O_4P_2^+B_2F_4$); complex **2b** ($C_{78.3}H_{79.46}B_2Cu\ F_8N_{11.15}O_2P_2$) is a crystal solvate with acetonitrile; two disordered acetonitrile molecules have a fractional occupancy; complex **3** ($C_{71}H_{67}Cl_{13}Mn_2N_6O_2P_2$) is a crystal solvate with chloroform; the structure was refined using the SQUEEZE procedure taking into account unknown solvents.

Evaluation of cytotoxic activity. The experiments were performed using the human cancer cell cultures M—HeLa clone 11 (epithelial cervical carcinoma, cell subline HeLa, clone M—HeLa) and HuTu80 (duodenum adenocarcinoma), which were obtained from the Russian Collection of Cell Cultures of the Institute of Cytology of the Russian Academy of Sciences (St. Petersburg, Russia), and the human normal liver cell line (Chang liver) from the Collection of the N. F. Gamaleya Research Institute of Epidemiology and Microbiology (Moscow). Tamoxifen and 5-fluorouracil (Sigma-Aldrich) were used as the reference compounds.

The cytotoxic effect of the compounds against the human cancer and normal cells was evaluated by counting the viable cells using the multifunctional Cytell Cell Imaging system (GE Healthcare Life Science, Sweden) and the Cell Viability BioApp application, which allows one to obtain accurate cell counts and viability estimations based on the fluorescence intensity. Two fluorescent dyes were used, which selectively penetrate the cell membranes and fluoresce at different wavelengths. The low-molecular-weight dye 4′,6-diamidine-2-phenylindole (DAPI) is able to pass through intact living cell membranes and stain the cell nuclei blue. The high-molecular-weight dye propidium iodide permeates only dead cells with damaged membranes, staining them orange. Therefore, the living cells are stained blue and the dead cells are stained orange. Propidium iodide and DAPI were purchased from Sigma-Aldrich.

The Igla minimum essential medium, produced by the M. P. Chumakov Institute of Poliomyelitis and Viral Encephalitis (PanEco company), supplemented with 10% fetal calf serum and 1% non-essential amino acids (NEAA). The cells were inoculated into Nunc 96-well plates at a dose of 10^5 cells mL^{-1} per well in the Igla medium (150 μL) and cultured for 24 h at 37 °C in a CO_2 incubator. Then the cul-

ture medium was withdrawn, and solutions (150 μL) of the tested compounds at specified dilutions were added to the wells. The dilutions of the compounds were prepared directly in the growth culture medium supplemented with 5% DMSO to improve the solubility. The cytotoxic effect of the tested compounds was evaluated at concentrations of 1—100 mmol L^{-1}. The concentrations of the compounds required to inhibit 50% cell growth (IC_{50}) were calculated using the MLA—Quest Graph™ IC_{50} Calculator AAT Bioquest, Inc, 25 July, 2019, https://www.aatbio.com/tools/ic50-calculator. The selectivity indices (SI) were calculated as the ratio of IC_{50} (the concentrations of compounds required to inhibit 50% cell growth in the experimental population) for the normal cells to IC_{50} for the cancer cells. All experiments were performed in triplicate.

Elemental analysis was carried out on a EuroVector-3000 analyzer (C, H) and manually by the pyrolysis of a weighed sample under an oxygen flow (P).

1,3-Dibenzhydryl-5-(pyridin-2-yl)-1,3,5- diazaphosphinane 5-oxide (L). Two equivalents of a 30% aqueous hydrogen peroxide solution (1.56 mmol, 0.16 mL) were added to a solution of diazaphosphorinane (0.78 mmol) in acetone (10 mL). The reaction mixture was stirred for 2 h at room temperature. The solvent was removed, and the residue was dried under reduced pressure ($2 \cdot 10^{-2}$ mBar) and recrystallized from ethanol, resulting in the formation of a white powder. The yield was 0.165 g (45%), m.p. 125 °C. ^{1}H NMR ($CDCl_3$), δ: 8.68 (d, 1 H, Py, J = 4.5 Hz); 8.08—8.03 (m, 1 H, Py); 7.80—7.73 (m, 1 H, Py); 7.39 (d, 4 H, *o*-C$\underline{H}_{APh}$, J = 7.3 Hz); 7.36—7.32 (m, 1 H, H, Py); 7.29 (d, 4 H, *o*-C$\underline{H}_{BPh}$, J = 7.3 Hz); 7.23—7.08 (m, 8 H, *m*-C$\underline{H}_{Ph}$); 7.14 (t, 2 H, *p*-C$\underline{H}_{APh}$, J = 7.4 Hz); 7.11 (t, 2 H, *p*-C$\underline{H}_{BPh}$, J = 7.4 Hz); 5.08 (s, 2 H, C_{Ph}—C$\underline{H}$—C_{Ph}); 3.83 (d, 1 H, N—C$\underline{H}_A$$H_B$—N, J =12.0 Hz); 3.59 (d, 1 H, N—CH_AC$\underline{H}_B$—N, J =12.0 Hz); 3.41 (d, 2 H, P—C$\underline{H}_{2(eq)}$—N, J = 14.1 Hz); 3.21 (d, 2 H, P—C$\underline{H}_{2(ax)}$—N, J = 14.1 Hz). ^{31}P{^{1}H} NMR ($CDCl_3$), δ: 18.3. ESI-MS, m/z (I_{rel} (%)): 530 $[M + H]^+$ (100), 552 $[M + Na]^+$ (17). IR (Nujol mulls), ν/cm^{-1}: 2925 (C—H), 2855 (C—H), 1576 (C=N), 1492, 1456, 1378, 1174 (P=O), 1053, 865, 841, 769, 751, 711, 699. Found (%): C, 76.98; H, 6.05; N, 7.96; P, 5.87. $C_{34}H_{32}N_3OP$. Calculated (%): C, 77.11; H, 6.09; N, 7.93; P, 5.85.

Synthesis of complexes 1—3 (general procedure). A solution of $CuCl_2 \cdot 2H_2O$ (0.16 mmol (for **1**)), $Cu(BF_4)_2 \cdot H_2O$ (0.17 mmol (for **2**)), or $MnCl_2$ (0.22 mmol (for **3**)) in EtOH (5 mL) was added to a solution of ligand **L** (0.33, 0.34, 0.22 mmol, respectively) in ethanol (5 mL), resulting in the formation of the green (**1**), blue (**2**), or transparent (**3**) reaction mixture. The solution was stirred for 12 h, and the solvent was removed under reduced pressure. The pale-green (**1**), blue (**2**), or white (**3**) solid residue was washed 2—3 times with diethyl ether, filtered off, dried under reduced pressure ($2 \cdot 10^{-2}$ mBar), and recrystallized from acetonitrile.

Bis[k^2-(*N,O*)-1,3-dibenzhydryl-5-(pyridin-2-yl)-1,3,5-diazaphosphorinane 5-oxide]dichlorocopper(II) (1). The yield was 0.15 g (39%), m.p. 149 °C. ESI-MS, m/z (I_{rel} (%)): 530 $[M - Cu - L - 2\ Cl + H]^+$ (100), 631 $[M - L - Cl]^+$ (10). IR (Nujol mulls), ν/cm^{-1}: 2921 (ν(C—H)), 2854 (ν(C—H)), 1463, 1377, 1234, 1168 (ν(P=O)), 1115, 1082, 1052, 1027, 911, 889, 708. Found (%): C, 68.40; H, 5.44; Cl, 5.95; Cu, 5.30; N, 7.07; P, 5.15. $C_{68}H_{64}Cl_2CuN_6O_2P_2$. Calculated (%): C, 68.42; H, 5.40; Cl, 5.94; Cu, 5.32; N, 7.04; P, 5.19.

Bis[k^2-(*N,O*)-1,3-dibenzhydryl-5-(pyridin-2-yl)-1,3,5-diazaphosphorinane 5-oxide]copper(II) tetrafluoroborate (2). The yield was 0.13 g (65%), m.p. 179 °C. ESI-MS, m/z (I_{rel} (%)):592 $[M - L - 2\ BF_4 + H]^+$ (43), 1121 $[M - 2\ BF_4 + H]^+$ (100). IR (Nujol mulls), ν/cm^{-1}: 2924 (ν(C—H)), 2854 (ν(C—H)), 1592 (ν(C=N)), 1493, 1456, 1377, 1290, 1269, 1229, 1152 (ν(P=O)), 1106, 1075 (ν(BF_4)), 1025, 914, 891, 854, 760, 748, 708. Found (%): C, 62.97; H, 4.95; Cu, 4.93; N, 6.44; P, 4.81. $C_{68}H_{64}B_2CuF_8N_6O_2P_2$. Calculated (%): C, 63.00; H, 4.98; Cu, 4.90; N, 6.48; P, 4.78.

Bis-μ-[k^2-(*N,O*)-1,3-dibenzhydryl-5-(pyridin-2-yl)-1,3,5-diazaphosphorinane 5-oxide]tetrachlorodimanganese(II) (3). The yield was 0.26 g (89%), m.p. 169 °C. MALDI-MS, m/z (I_{rel} (%)): 1149 $[M - 3\ Cl + H]^+$ (100). IR (Nujol mulls), ν/cm^{-1}: 2955 (ν(C—H)), 2927 (ν(C—H)), 2854 (ν(C—H)), 1583 (ν(C=N)), 1492, 1455, 1377, 1262, 1153 (ν(P=O)), 1130, 1087, 1048, 1027, 764, 745, 706. Found (%): C, 61.73; H, 4.95; Cl, 10.78; Mn, 8.31; N, 6.45; P, 4.70. $C_{68}H_{64}Cl_4Mn_2N_6O_2P_2$. Calculated (%): C, 62.30; H, 4.92; Cl, 10.82; Mn, 8.38; N, 6.41; P, 4.73.

The measurements were carried out using the equipment of the Assigned Spectral-Analytical Center of Shared Facilities for Study of Structure, Composition and Properties of Substances and Materials of the FRC Kazan Scientific Center of the Russian Academy of Sciences.

No human or animal subjects were used in this research.

The authors declare no competing interests.

References

1. U. Ndagi, N. Mhlongo, M. Soliman, *Drug Des. Dev. Ther.,* 2017, **11**, 599; DOI: 10.2147/DDDT.S119488.
2. J.-X. Liang, H.-J. Zhong, G. Yang, K. Vellaisamy, D.-L. Ma, C.-H. Leung, *J. Inorg. Biochem.,* 2017, **177**, 276; DOI: 10.1016/j.jinorgbio.2017.06.002.
3. T. Johnstone, K. Suntharalingam, S. Lippard, *Chem. Rev.,* 2016, **116**, 3436; DOI: 10.1021/acs.chemrev.5b00597.
4. V. Brabec, O. Hrabina, J. Kasparkova, *Coord. Chem. Rev.*, 2017, **351**, 2; DOI: 10.1016/j.ccr.2017.04.013.
5. P. Starha, J. Vanc, Z. Travnicek, *Coord. Chem. Rev.*, 2019, **380**, 103; DOI: 10.1016/j.ccr.2018.09.017.
6. A. Matesanz, C. Hernandez, A. Rodriguez, P. Souza, *Dalton Trans.*, 2011, **40**, 5738; DOI: 10.1039/C1DT10212E.
7. A. Barve, A. Kumbhar, M. Bhat, B. Joshi, R. Butcher, U. Sonawane, R. Joshi, *Inorg. Chem.*, 2009, **48**, 9120; DOI: 10.1021/ic9004642.
8. C. Santini, M. Pellei, V. Gandin, M. Porchia, F. Tisato, C. Marzano, *Chem. Rev.,* 2014, **114**, 815; DOI: 10.1021/cr400135x.

9. M. Porchia, M. Pellei, F. Bello, C. Santini, *Molecules*, 2020, **25**, 5814; DOI: 10.3390/molecules25245814.
10. G. Barone, A. Terenzi, A. Lauria, A.-M. Almerico, J. Leal, N. Busto, B. Garcia, *Coord. Chem. Rev.*, 2013, **257**, 2848; DOI: 10.1016/j.ccr.2013.02.023.
11. H. Wang, M. Sorolla II, X. Wang, A. Jacobson, H. Wang, A. Pillai, *Transition Met. Chem.,* 2019, **44**, 237; DOI: 10.1007/s11243-018-0288-3.
12. I. A. Lutsenko, M. A. Kiskin, K. A. Koshenskova, P. V. Primakov, A. V. Khoroshilov, O. B. Bekker, I. L. Eremenko, *Russ. Chem. Bull.*, 2021, **70**, 463; DOI: 10.1007/s11172-021-3109-3.
13. C. Freidline, R. Tobias, *Inorg. Chem.*, 1966, **5**, 354; DOI: 10.1021/ic50037a006
14. T. Iiyama, M. Chikira, T. Oyoshi, H. Sugiyama, *J. Biol. Inorg. Chem.*, 2003, **8**, 135; DOI: 10.1007/s00775-002-0398-3.
15. R. Chen, C.-S. Liu, H. Zhang, Y. Guo, X.-H. Bu, M. Yang, *J. Inorg. Biochem.*, 2007, **101**, 412; DOI: 10.1016/j.jinorgbio.2006.11.001.
16. Y.-L. Wang, Y.-C. Liu, Z.-S. Yang, G.-C. Zhao, *Bioelectrochemistry*, 2004, **65**, 77; DOI: 10.1016/j.bioelechem.2004.07.002.
17. S. Tardito, O. Bussolati, F. Gaccioli, R. Gatti, S. Guizzardi, J. Uggeri, L. Marchiò, M. Lanfranchi, R. Franchi-Gazzola, *Histochem. Cell Biol.*, 2006, **126**, 473; DOI: 10.1007/s00418-006-0183-4.
18. N. S. Rukk, L. G. Kuzmina, G. A. Davydova, G. A. Buzanov, S. K. Belus, E. I. Kozhukhova, V. M. Retivov, T. V. Ivanova, V. N. Krasnoperova, B. M. Bolotin, *Russ. Chem. Bull.*, 2020, **69**, 1394; DOI: 10.1007/s11172-020-2914-4.
19. E.-J. Gao, Y. Zhang, L. Lin, R.-S. Wang, L. Dai, Q. Liang, M.-C. Zhu, M.-L. Wang, L. Liu, W.-X. He, Y.-J. Zhang, *J. Coord. Chem.*, 2011, **64**, 3992; DOI: 10.1080/00958972.2011.634910.
20. K. Trigulova, A. Shamsieva, R. Faizullin, P. Lonnecke, E. Hey-Hawkins, A. Voloshina, E. Musina, A. Karasik, *Russ. J. Coord. Chem.*, 2020, **46**, 600; DOI: 10.1134/S1070328420090055.
21. A. Karasik, E. Musina, A. Balueva, I. Strelnik, O. Sinyashin, *Pure Appl. Chem.*, 2017, **89**, 293; DOI: 10.1515/pac-2016-1022.
22. B. A. Arbuzov, O. A. Erastov, G. N. Nikonov, T. A. Zyablikova, D. S. Yufit, Yu. T. Struchkov, *Bull. Acad. Sci. USSR, Div. Chem. Sci.*, 1981, **30**, 1539.
23. A. V. Shamsieva, K. R. Trigulova, R. R. Fayzullin, V. V. Khrizanforova, Yu. G. Budnikova, E. I. Musina, A. A. Karasik, *Russ. Chem. Bull.*, 2018, **67**, 1206; DOI: 10.1007/s11172-018-2203-7.
24. A. Artem´ev, M. Davydova, A. Berezin, T. Sukhikh, D. Samsonenko, *Inorg. Chem. Front.*, 2021, **8**, 2261; DOI: 10.1039/d1qi00036e.
25. A. Artem´ev, M. Davydova, A. Berezin, V. Brel, V. Morgalyuk, I. Bagryanskaya, D. Samsonenko, *Dalton Trans.*, 2019, **48**, 16448; DOI: 10.1039/c9dt03283e.
26. A. Berezin, M. Davydova, I. Bagryanskaya, O. Artyushin, V. Brel, A. Artem´ev, *Inorg. Chem. Commun.*, 2019, **107**, 107473; DOI:10.1016/j.inoche.2019.107473.
27. D. Montagner, B. Fresch, K. Browne, V. Gandin, A. Erxleben, *Chem. Commun.*, 2017, **53**, 134; DOI: 10.1039/C6CC08100B.
28. A. Voloshina, S. Gumerova, A. Sapunova, N. Kulik, A. Mirgorodskay, A. Kotenko, T. Prokopyeva, V. Mikhailov, L. Zakharova, O. Sinyashin, *Biochi. Biophys. Acta*, 2020, **1864**, 129728; DOI: 10.1016/j.bbagen.2020.129728.
29. G. Sheldrick, *Acta Crystallogr., Sect. A*, 2015, **71**, 3; DOI:10.1107/S2053273314026370.
30. G. Sheldrick, *Acta Crystallogr., Sect. C*, 2015, **71**, 3; DOI: 10.1107/S2053229614024218.
31. A. Spek, *Acta Crystallogr.*, *Sect. C*, 2015, **71**, 9; DOI: 10.1107/S2053229614024929.
32. A. Spek, *Acta Crystallogr.*, *Sect. D*, 2009, 65, 148; DOI: 10.1107/S090744490804362X.
33. C. Macrae, I. Sovago, S. Cottrell, P. Galek, P. McCabe, E. Pidcock, M. Platings, G. Shield, J. Stevens, M. Towler, P. Wood, *J. Appl. Crystallogr.*, 2020, **53**, 226; DOI: 10.1107/S1600576719014092.

Received March 29, 2022;
in revised form April 29, 2022;
accepted May 4, 2022